

1 **Developing Integrated PBPK/PD Coupled mechanistic pathway**  
2 **model (miRNA-BDNF): an approach towards System**  
3 **toxicology**

4

5 Raju Prasad Sharma, Marta Schuhmacher, Vikas Kumar\*

6

7

8

9 *Center of Environmental Food and Toxicological Technology (TecnATox),*  
10 *Departament d'Enginyeria Química, Universitat Rovira i Virgili,*  
11 *Tarragona, Catalonia, Spain*

12

13

14

15

16

17

18 \* Corresponding author: Environmental Engineering Laboratory, Departament d'Enginyeria  
19 Química, Universitat Rovira i Virgili, Tarragona, Catalonia, Spain. Tel.: +34977558576.

20 *E-mail address:* vikas.kumar@urv.cat

21

22

23 **Abstract:**

24 Integration of a dynamic signal transduction pathway into the tissue dosimetry model is  
25 a major advancement in the area of computational toxicology. This paper illustrates the  
26 ways to incorporate the use of existing system biological model in the field of  
27 toxicology via its coupling to the Physiological based Pharmacokinetics and  
28 Pharmacodynamics (PBPK/PD) model. This expansion framework of integrated  
29 PBPK/PD coupled mechanistic system pathway model can be called as system  
30 toxicology that describes the kinetics of both -the chemicals and -biomolecules, help us  
31 to understand the dynamic and steady-state behaviors of molecular pathways under  
32 perturbed condition. The objective of this article is to illustrate a system toxicology  
33 based approach by developing an integrated PBPK/PD coupled miRNA-BDNF pathway  
34 model and to demonstrate its application by taking a case study of PFOS mediated  
35 neurotoxicity. System dynamic involves miRNA-mediated BDNF regulation, which  
36 plays an important role in the control of neuronal cell proliferation, differentiation, and  
37 survivability.

38 **Key words:** PBPK/PD, miRNA, BDNF, Neuroendocrine, System biology, PFOS

## 39 1. Introduction

40 In the field of quantitative risk assessment, a journey of classical dose-response models  
41 is categorized into different classes for the better quantification and estimation of early  
42 possible risk (Andersen et al., 2005). These include –a) Physiological based  
43 pharmacokinetic and pharmacodynamic modeling (PBPK) for the quantification of  
44 internal biophase concentrations in different tissues, b) pharmacodynamics (PD) model  
45 quantifies the interactions of chemicals with target biomolecules c) System Biology  
46 describes the dynamic relationship of biological components for a robust physiological  
47 response. Perturbation of these biological components can be quantified through the  
48 integration of PBPK/PD model into the system biological models providing a predictive  
49 tool for measuring toxicological impact at the cellular and biomolecular level (Andersen  
50 et al., 2005; Gohlke et al., 2005; Zhao and Ricci, 2010).

51 The PBPK model in the area of dosimetry risk assessment has been widely accepted and  
52 applied and it is among the top priority tool recommended in the vision of toxicity  
53 testing in the 21<sup>st</sup> century (Andersen and Krewski, 2009). PBPK model has been  
54 extended to develop the PBPK/PD for certain pesticides (Timchalk et al., 2002;  
55 Foxenberg et al., 2011). The integration of PD was generally done with the  
56 quantification of the response variable (biomarker) effect of an interaction of a chemical  
57 (biophase concentration estimated by PBPK) with a target biomolecule (mainly  
58 receptors). But it has a certain limitation such as lack of robust biology (biomarker  
59 relation to endpoint), and very often the endpoints are specifically remained single  
60 explanatory biomarker. Coupling of PBPK/PD model and system biology together can  
61 enlighten the effect of changes in key biomolecules considering the whole biological  
62 system. System biology comprising of genomics, metabolomics, and proteomics which  
63 rationalizes the functional interaction of biological components in a time-dependent  
64 fashion (Aderem, 2005; Kitano, 2002). Thus, it could be useful in system toxicology for  
65 understanding the altered biological pathway due to chemical induced perturbation of  
66 certain key biomolecule in a system, illustrating differences from normal pathway  
67 (Arrell and Terzic, 2010; Auffray et al., 2009; Hood et al., 2004; Kell, 2006).  
68 Understanding the biomolecular mechanisms are of great interest to identify the  
69 toxicological effects at the very early stages of the disease (toxicological response).  
70 However, often we lack sufficient information to link chemically perturbed biological  
71 components (molecular biomarker) to an altered biological system. This lead to the use  
72 of the simplified dose-response model (simple PD) to predict the adverse outcome  
73 (disease) for a target chemical (Calabrese and Baldwin, 2003). In the field of toxicology,  
74 there is limited use of these system biology models (Waters et al., 2003). The wide use  
75 of system toxicology in human environmental risk assessment has a time lag in  
76 comparison with pharmaceuticals science as it lacks experimental data, has complex  
77 interaction pathways of environmental chemicals than the target specific drugs, and low  
78 commercial priority of applied toxicological science.

79 Recently use of the integrated PBPK/PD models in a field of environmental toxicology,  
80 enables development of a quantitative biologically based risk model which increases our  
81 understanding towards the relationship between tissue bio-phase concentration of  
82 chemicals and endogenous biomolecule (Timchalk et al., 2002; Foxenberg et al., 2011).  
83 Furthermore, signaling pathways could be used as an extension of PBPK/PD, given  
84 dynamic interactions of chemicals with biological components are known, the first step  
85 towards system toxicology (Bhattacharya et al., 2012; Gim et al., 2010). It has benefits  
86 such as: easy to implement if the signaling pathway already developed, often data from

87 the dose-response experiments for known biomolecules can be used, a good step to use  
88 Adverse Outcome Pathways (AOPs) knowledge to develop the generic PBPK/PD  
89 model for multi-species and multi-chemicals.

90 Neuroendocrine or neurotrophins such as nerve growth factors, BDNF and  
91 neurotrophin-3 are proteins, basically processed and secreted in constitutive and  
92 regulatory fashion in non-neuron, neurons and neuroendocrine cells (Lu, 2003; Mowla  
93 et al., 1999). Among them, BDNF is immensely expressed and extensively scattered  
94 than other neurotrophins, and play an important role in neuronal survival and  
95 differentiation (Boulle et al., 2012; Michael et al., 1997; Murer et al., 2001). BDNF  
96 binds with a Tropomyosin receptor kinase B (TrkB) presents on the neuronal cell  
97 surface causing sequential activation of following pathways such as Mitogen-activated  
98 protein kinases (MAPKs), Extracellular-signal-regulated kinase (ERK), and Protein  
99 kinase B (AKT) that are mainly involved in differentiation and survivability of neurons  
100 (Michael et al., 1997; Murer et al., 2001 Bursac et al., 2010; Boulle et al., 2012). It has  
101 been seen that reduced BDNF protein and mRNA expression is linked with several  
102 neurological disorders such as Alzheimer's and Parkinson's (Bursac et al., 2010).  
103 Moreover, dopaminergic, GABAergic, cholinergic, and serotonergic neurons are known  
104 to require BDNF for their proper development and survival (Lipsky and Marini, 2007;  
105 Murer et al., 2001), signifies BDNF as an important biomarker for neurodevelopmental  
106 function.

107 It has been reported that miRNA regulates the synthesis of BDNF via  
108 posttranscriptional modification of BDNFmRNA (Caputo et al., 2011; You et al., 2016).  
109 Muiños-Gimeno et al., (2011) reported the involvement of miRNA-22 associated panic  
110 disorders in the Spanish and North European population. Later, the transcriptomic  
111 analysis studied by Li et al., (2015) in SH-SY5Y cell line also found the involvement of  
112 miRNA-22 dependent decrease in the BDNF level and neuronal cell survivability. The  
113 miRNAs are turning out to be significant regulators of mRNAs and the related proteins.  
114 In this proposed study, miRNA (micro-RNA) regulated BDNF (Brain- derived  
115 neurotropic factor) and its effect on neuronal survivability mechanisms was selected for  
116 the development of the mechanistic base model. Perfluorooctanesulfonic acid (PFOS)  
117 was selected as a case study to illustrate the ways to incorporate the use of system  
118 biological model in the field of toxicology via Pharmacodynamic coupled tissue  
119 dosimetry model(PBPK/PD).

## 120 **Case studies on PFOS**

121 PFOS is well recognized among industrial chemicals that can easily cross the BBB  
122 (blood brain barrier) (Sato et al., 2009) and its exposure was related to several  
123 developmental neurotoxicity effects (Johansson et al., 2008; Yang et al., 2015; Goudarzi  
124 et al., 2016; Vuong et al., 2016) . For instance, it was found that PFOS exposure to  
125 zebrafish causing an alteration in the expression of more than 40 different type of  
126 miRNAs allied with the developmental toxicities (Zhang et al., 2011). The several  
127 mechanisms were hypothesized for the PFOS causing development neurotoxicity  
128 disorders such as oxidative stress, altering neurotransmitters level and upregulation and  
129 downregulation of apoptotic and pro-survival factors from various animals and cell line  
130 studies (Long et al., 2013; Chen et al., 2014; Yu et al., 2016). In a recent study, it was  
131 found that PFOS can decrease the neuronal cell survivability by altering the level of  
132 miRNA in human neuroblastoma cell line(Li et al., 2015). This could be an important  
133 mechanism of PFOS as it has been seen that miRNAs regulate the proteins level by

134 regulating their mRNAs expression level. The purpose of our model is to test the  
135 hypothesis that PFOS perturbed the miRNA affecting neuronal survivability via  
136 regulating BDNF at mRNA level. The human dosimetry study has shown the longer  
137 residence time of PFOS inside the body and relatively higher concentration in the brain  
138 tissue than comparing to other perfluoroalkyl substances (PFASs) (Fabrega et al., 2014).  
139 Furthermore, its continuous exposure and potential to cross the BBB could put the  
140 humans at high risk of neurodevelopmental disorders which is in consonance with  
141 recently published paper related to neurotoxicity of PFOS (Yang et al., 2015; Vuong et  
142 al., 2016). The PFOS PBPK model has been well developed previously by Fabrega et  
143 al., (2014) that predicts internal tissue dose. However, for a better understanding of  
144 toxicological mechanisms in the context of risk assessment, we would need one more  
145 step towards the system toxicology. This gap could fill by coupling integrated  
146 PBPK/PD model into a mechanistic system model.

147 The objective of this study was the development of a mechanistic pathway system  
148 (miRNA-BDNF mRNA- BDNF- cell survivability) model and coupling of above model  
149 with a PBPK/PD taking a case study of the PFOS induced neurotoxicity.

150

## 151 **2. Materials and Methods**

### 152 **2.1. miRNA-mRNA-BDNF-cell survival mechanistic pathway (figure 1)**

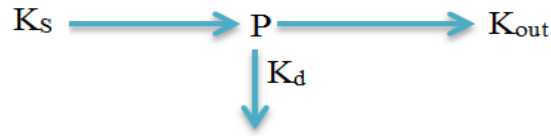
153 Generally, miRNA post-transcriptionally regulates the protein molecule via binding at  
154 3'UTR of mRNA (Perruisseau-Carrier et al., 2011). It has been found that miRNA  
155 decreases the level of BDNF either via degradation of mRNA or facilitating ribosome  
156 induced silencing complex formation with mRNA (RISCm) (Bartel, 2004; Djuranovic  
157 et al., 2011). The other mechanism involves miRNA inhibits the BDNF regulation by  
158 downregulating the expression of cyclic response element-binding protein (CREB)  
159 (Caputo et al., 2011; You et al., 2016). Nonetheless, the numbers of the regulatory  
160 pathways have been proposed (Zeng et al., 2011; Sandhya et al., 2013; York, 2015).  
161 Moreover, a study on population affected with neuronal disorders showed an inverse  
162 relationship between miRNA and BDNF level (Muiños-Gimeno et al., 2011)  
163 strengthens the evidence of regulation of BDNF via miRNA. BDNF dependent cell  
164 survival pathways can be extremely important from a regulatory perspective. The  
165 relationship between BDNF concentration and cell survival are quite well known via the  
166 dose-response curve obtained from the in-vitro cell line study (O'Leary and Hughes,  
167 1998). Nevertheless, intermediate molecular signaling pathways are prevailed in-  
168 between the binding of BDNF with TrkB receptors to the effects on the neuronal cell.  
169 This involves activation of MAPK/ERK and AKT-PI3K pathways that increase the  
170 neuronal survival and differentiation process via increasing expression of CREB  
171 (Michael et al., 1997; Murer et al., 2001 Bursac et al., 2010; Boulle et al., 2012). The  
172 conceptual diagram is provided in figure 1.

#### 173 **2.1.1. miRNA regulatory BDNF pathway model**

174 The regulatory pathway of BDNF involves different intermediate biomolecules.  
175 However, in this study, the generic miRNA-BDNF pathway was adapted from the  
176 previously published work of Wang et al., (2010) to developed exclusively miRNA  
177 regulatory BDNF model. The whole pathways are modeled by applying mass balance  
178 equation based on reaction kinetics applying ordinary differential equations. This  
179 allows the estimation of a biomolecule given the model parameter corresponds to the  
180 reaction rates. BDNF is the output of the miRNA-BDNF model, which was then used as

181 an input for the estimation of neuronal survival. The generic form of the system  
 182 dynamic model is as follow:

183



184

185 Where  $K_s$  is synthesis rate constant for the endogenous molecules,  $P$  is the  
 186 concentration of an endogenous molecule,  $K_d$  is the degradation rate constant,  $K_{out}$  is  
 187 the dissipation rate constant of  $P$  available for the synthesis of the subsequent  
 188 endogenous molecule. Following this schematic, concentration of endogenous  
 189 biomolecules is estimated by the following differential equation;

190 
$$\frac{d}{dt}(P) = K_s - K_d * P - K_{out} * P \quad \text{Eq. (1)}$$

191

192 **2.1.2. BDNF - cell survival Emax model-**

193 To simplify the model, we have applied hills sigmoid equations to get the output of the  
 194 neuronal survival by applying  $E_{max}$  and  $EC_{50}$  value of BDNF for neuronal cell  
 195 survival from experimental data (O’Leary and Hughes, 1998). The percentage of cell  
 196 survivability with respect to BDNF concentration was estimated by the use of sigmoid  
 197 Emax model applying the following equations;

198 
$$\text{Cell survivablity} = E_0 + ((E_{max} * C^n) / (EC_{50} + C^n)) \quad \text{Eq. (2)}$$

199 Where, Cell survivability = percentage of cell survivability as function of BDNF conc.,  
 200  $E_0$  = baseline response,  $E_{max}$  = maximum response,  $C$ = BDNF concentration,  $EC_{50}$ =  
 201 concentration at which BDNF shows 50% response of  $E_{max}$ ,  $n$ = hill coefficient

202 This developed Emax model was integrated into indirect response model eq. (3) that  
 203 provides the neuronal cell survivability as a function of time. More details on indirect  
 204 response models can be found in Bonate, (2011).

205 
$$\frac{d}{dt} \text{Cell survivablity} = k_{out\_BDNF} * \text{cell survivablity} - kd * \text{cell survivablity}(t) \quad \text{Eq. (3)}$$

207 Where  $\frac{d}{dt}$  Cell survivability = percentage of cell survivability in the time domain,  
 208  $k_{out\_BDNF}$  is BDNF conc. assumed to be responsible for neuronal cell survivability,  
 209  $kd$  is the degradation rate of the neuronal cell.

210 **2.2. PFOS PBPK (a case study)**

211 The PBPK model of PFOS was adapted from the previously published model (Fabrega  
 212 et al., 2014). The concentration of PFOS in a brain considered as the effective target  
 213 dose (target tissue dosimetry), considering the brain as a target organ in relation to  
 214 potential neurodevelopment deficit disorders. PBPK model generates time course of  
 215 PFOS concentration in the brain, which is used as input for the mechanistic pathway

216 model. At the end, integration of the PBPK model of PFOS into the mechanistic BDNF  
217 –cell survivability model analyzes the perturbation of PFOS on the whole pathway  
218 results in decreased in neuronal cell survival rate. The conceptual model for this  
219 integration is provided in figure 2.

220 Concentrations in the respective compartment (muscle, richly perfused, fat, kidney,  
221 Brain and liver) are estimated by applying the following equation:

$$\frac{dC_i}{dt} = \frac{Q_i \times \left( C_a - \frac{C_i}{K_{i:p}} \right)}{V_i} \quad \text{Eq. (4)}$$

224

225 Where,  $C_i$  is the concentration in the tissue  $i$  (ng/L),  $Q_i$  is the blood flow in the tissue  $i$   
226 (L/h),  $C_a$  is the arterial concentration (ng/L),  $K_{i:p}$  is the partition coefficient of tissue  $i$ ,  
227 and  $V_i$  is the volume of the tissue  $i$  (L). Detail description of PBPK model can be found  
228 in our other publications (Fabrega et al., 2014; Fàbrega et al., 2016).

229 All the physiological, Physicochemical parameters and model equations for the PBPK  
230 are provided in the Annex-I

### 231 **2.3. IVIVE for dose Equivalency**

232 In-vitro in-vivo extrapolation (IVIVE) method was used in order to estimate the oral  
233 equivalent dose from the given in-vitro dose. It has an assumption that the in-vitro area  
234 under the curve (AUC), calculated by multiplying dose with the total duration of  
235 exposure, would be similar with the AUC of target in-vivo organ (in this case Brain).

236 Li et al., (2015) in-vitro studies on SH-SY5Y cell line was selected, where a decrease in  
237 neuronal cell survivability found to depend on miRNA and BDNF. In Li et al., an  
238 experiment they used 12 in-vitro doses (6 doses each for 24hr and 48 hr) for that  
239 corresponding in vivo doses was determined. The assumption was made that in-vitro  
240 doses are equivalent to internal target concentration (brain). For the reconstructing  
241 equivalent oral dose, the AUC value was calculated for each in-vitro conc., based on  
242 their duration of treatment (In this case 24hr and 48 hr). The conceptual schematic for  
243 dose reconstruction is provided in figure 3. The calculated AUC was assumed to be  
244 equivalent with in-vivo AUC brain. Dose reconstruction approach has been used, so that  
245 the given equivalent oral dose will provide the AUC in the brain that matches the AUC  
246 for the 12 different in-vitro doses (6 for 24hr and 6 for 48hr), a similar approach has  
247 been used in the previous study (Thiel et al., 2017). The oral equivalent doses were  
248 estimated to be way higher, as the PFOS concentration reaching to the brain was found  
249 to be relatively very low (Fabrega et al., 2014; Fàbrega et al., 2016). The estimated oral  
250 equivalent doses for the corresponding in-vitro doses are provided in Table 1.

### 251 **2.4. Integrated PBPK/PD coupled miRNA-BDNF-cell survival pathway**

252 Coupling of PBPK to mechanistic miRNA-BDNF pathway model has been done with  
253 the integration of brain PFOS concentration as a target input that perturbs key  
254 component miRNA of the pathway. The interaction of the PFOS with the miRNA has  
255 done based on empirical evidence but the mechanism behind the interaction is still not  
256 clear. The coupling was done by applying stimulatory Emax model that assumes PFOS  
257 increase the concentration of miRNA via increasing their synthesis rate. Finally the

258 output we measured as a percentage of neuronal survival rate considering two scenarios;  
259 with and without PFOS exposure. The conceptual diagram is provided in figure 4.

260 The integration of PFOS into the BDNF pathway is done by indirect pharmacodynamic  
261 interaction model with the following equation;

$$262 \quad \frac{d}{dt}(miRNA) = K_{in_{miRNA}} * \left(1 + \frac{Emax * C}{EC_{50} + C}\right) - K_{out_{miRNA}} * miRNA_0 \quad \text{Eq. (5)}$$

263 Where,  $K_{in_{miRNA}}$  = synthesis rate constant of miRNA,  $K_{out_{miRNA}}$  = dissipation rate of  
264 miRNA,  $miRNA_0$  = initial value of miRNA,  $Emax$  = maximum response for miRNA,  $C$   
265 = brain concentration of PFOS,  $EC_{50}$  = concentration at which PFOS shows 50%  
266 response of  $Emax$ .

267

## 268 **2.5 Model parameterization**

269 The mi-RNA-mRNA-Protein pathway parameters were taken from the previously  
270 published model (Wang et al., 2010). Specifically, BDNF protein synthesis rate was  
271 used instead of generic protein synthesis. There was no BDNFmRNA synthesis rate  
272 data available in the literature and for that generic BDNFmRNA rate constant was used.  
273 BDNF synthesis rate was taken from the Castillo et al., (1994) and Menei et al., (1998).  
274 Furthermore, the synthesis rate was scaled accounting number of neuronal cells to the  
275 whole body per kg weight nmol/hr/kg<sup>(0.75)</sup>. The degradation rate of BDNF was  
276 parameterized from half- life by using the following relationship: degradation rate =  
277  $\ln 2/t_{1/2}$ .

278 For the quantification of neuronal survival against BDNF exposure, the required  $Emax$   
279 and  $EC_{50}$  parameters for establishing sigmoid  $Emax$  model were taken from O'Leary  
280 and Hughes,(1998). The  $Emax$  and  $EC_{50}$  values for the reaction are implemented as  
281 such as these parameters tend to have a similar trend across species (Gatzeva-topalova  
282 et al., 2011). PBPK parameters for the PFOS were used from the previously published  
283 article (Fabrega et al., 2014). The dynamic interaction data for the PFOS to miRNA,  
284 such as  $EC_{50}$  estimated from Li et al., (2015). All the parameters that were used for  
285 developing mechanistic model are provided in Table 2. All the model equations for the  
286 mechanistic and integrated PBPK/PD-mechanistic models are provided in the Annex-I

287

## 288 **3. Results**

289 The simulation of the model is divided into two parts; the first simulation of a PBPK  
290 and a mechanistic system pathway model individually to get the base model. Later  
291 simulation of integrated PBPK/PD coupled mechanistic model (system toxicology) was  
292 done. The integration of Pharmacodynamic interaction between PFOS and target  
293 biomolecule was done by using indirect response model. The equivalent exposure doses  
294 for the PFOS were extrapolated from the in-vitro study of Li et al., (2015). Neuronal  
295 survivability was chosen as an end point biomarker for the model and mapping of in-  
296 vitro data (neuronal survivability) to in-vivo was done based on linear interpolation  
297 method. The PFOS PBPK model codes are provided by Fabrega et al., (2014) which  
298 was used in this paper to simulate PBPK model.

299 The mechanistic system model simulations were performed for the miRNA-BDNF  
300 signaling pathway and the resulting time course of BDNF was recorded as model  
301 output. The output of the BDNF time course data was used for performing the  
302 simulation to get the percentage of cell survivability by applying indirect sigmoid  
303 response model. This part of simulation results recorded as the normal baseline value  
304 for the model. The figure 6 (base model of the mechanistic pathway) showed the  
305 baseline value of important endogenous biomolecules like miRNA, BDNF, RISC(RNA-  
306 induced silencing complex), RISCm (complex form between BDNFmRNA and RISC)  
307 and percentage of neuronal cell survivability. The mechanistic system model has  
308 optimized to achieve the maximum neuronal cell survivability steady state which is in  
309 compliance with experiment data given by Gillespie et al., (2003). The model has been  
310 simulated for 20 days in order to achieve the steady state. The miRNA regulation of  
311 BDNF via forming a complex between RISC and BDNFmRNA called RISCm has been  
312 documented can be seen in the base model figure number 6 which is in compliance with  
313 Wang et al., (2010) model. This complex formation between RISC and BDNFmRNA  
314 was enhanced by the miRNA resulting in a decrease of BDNF protein synthesis. The  
315 RISC complex binds with the mRNA at the 3' UTR and inhibits its further translation to  
316 protein. The base model also able to capture the phenomena of regulating BDNF protein  
317 by miRNA considered to be one of the important biological processes. The behavior of  
318 model curve for BDNF and cell survival are in a similar trend, which was also observed  
319 in in-vivo experiments (Rodríguez-Tébar et al., 1992; O'Leary and Hughes, 1998;  
320 Fletcher et al., 2008). The model shows BDNF maintains cell survivability at the steady  
321 state level of around 95 percent. In Figure (6), a sudden drop in the cell survivability to  
322 40 percent level could be explained considering the lag time in the attainment of BDNF  
323 steady state level. The simulation of the base model (Figure 6) shows that model able to  
324 retain the steady state for cell survivability at 95% once BDNF attained a steady state.  
325 A similar observation was reported by Gillespie et al., (2003) experimental study that  
326 survivability of neuron in presence and absence of BDNF were 90 percent and 40  
327 percent respectively.

328 The PBPK model simulation was carried out for the PFOS for the estimated oral  
329 equivalent dose (12 doses) given as a single dose. Figure 5 shows the simulation of the  
330 internal target tissue (brain) concentration of PFOS with 12 different dose levels  
331 providing different C<sub>max</sub> in dose dependent manner over the time period. The dose was  
332 given at the 240hr as shown in figure 6 when the mechanistic base model reaches steady  
333 state.

334 The coupling of PBPK into the mechanistic model was done by fitting in-vitro data,  
335 estimated from Li et al., (2015) study, via applying E<sub>max</sub> sigmoid model. The  
336 developed coupled PBPK/PD-mechanistic model quantifies the dynamic of the  
337 endogenous biomolecular concentration of different species at the different level of  
338 PFOS exposure that perturb key components of the system (in the miRNA model). The  
339 interaction of the PFOS to the given pathway was modeled by implementing indirect  
340 sigmoid response model **Eq. (5)** for PFOS-miRNA interaction. Consequently, dynamic  
341 changes in miRNA level as a function of PFOS concentration over time was observed  
342 (figure 7). The PFOS alter the steady state of all biological components involved in the  
343 pathway via stimulating input of miRNA disturbing whole mechanistic pathway. The  
344 integrated model was simulated for 12 different in-vitro equivalent in-vivo doses  
345 describing the whole system as one unit rendering time course of endogenous  
346 concentration after exposure to environment chemicals distinct from normal condition  
347 (Base model).

348 The figure 7, 8, 9 and 10 shows the effect of a chemical on the endogenous biomolecule  
349 concentration (miRNA, RISCm, BDNF) and cell survivability (in percentage)  
350 respectively over the time period. Figure 7 illustrates the dose depended effects of  
351 PFOS on miRNA level following single exposure to PFOS (dose given at 240hr).  
352 Figure 8 illustrates the increase in the formation of the RISCm complex after the PFOS  
353 exposure. The increase of RISCm complex concentration is due to increase of miRNA  
354 level which can be considered as an indirect action of PFOS. The highest level of  
355 miRNA is observed at t<sub>max</sub> (time point of C<sub>max</sub>) of PFOS and, with the elimination of  
356 PFOS from the system, shifting of miRNA level to steady state concentration at the  
357 level higher than baseline concentration was observed. Consequently, a decrease in the  
358 level of BDNF (figure 9) was noted as increase miRNA level facilitates the formation of  
359 the RISCm (figure 8), posttranscriptional regulatory mechanism of miRNA (explained  
360 in 2.1). With the increase in dose level, the difference between base steady state  
361 concentration and shifted steady state concentration was higher that can be seen in  
362 figure 7, 8, 9 and 10. Figure 10, illustrates the time vs neuronal survivability that  
363 describes the effect of PFOS over time as an end point biomarker.

## 364 **5. Discussion and Conclusions**

365 In this study, an attempt was made for the development of an integrated PBPK/PD  
366 coupled mechanistic model that allows assessing or characterizing the potential impact  
367 of environmental chemicals on a biological system. An Integrated PBPK/PD PFOS  
368 model and a mechanistic (miRNA-BDNF-neuronal survival) system model were  
369 evaluated individually. The generic mi-RNA model was adapted with a modification in  
370 BDNF as a target output protein. The regulation of BDNF involves several pathways  
371 among which miRNA-dependent pathway is an important one. The endogenous level of  
372 BDNF has an important effect on the survivability of neurons. For example principal  
373 hierarchy of BDNF signaling and consequently activation of MAPK/ERK/AKT  
374 pathway is well understood (Michael et al., 1997; Murer et al., 2001 Bursac et al., 2010;  
375 Boulle et al., 2012), but how these events control cellular survival are not well  
376 understood. The reported relation between chemical exposure and significant changes in  
377 BDNF level, consequently neuronal adverse outcomes, made a plausible argument of  
378 considering BDNF as a good biomarker. To keep biological plausibility intact in our  
379 mathematical expression, we restrict our model to the miRNA-BDNF pathway, and  
380 later linking it to the cell survivability as a function of the time course of BDNF  
381 concentration by applying E<sub>max</sub> model. The developed mechanistic model shows  
382 miRNA-dependent regulation of BDNF which is a natural phenomenon of this model  
383 retaining the regulatory mechanism of miRNA on BDNF. The mechanistic base model  
384 (figure 6) well predicted the percentage of cell survivability as a function of BDNF  
385 concentration. The PBPK model was used to estimate the internal target dose of  
386 chemicals. The output of PBPK in target organ is used as input for the mechanistic  
387 system model providing integrated coupled PBPK/PD-mechanistic system model. This  
388 will describe the whole system as one unit rendering time course of endogenous  
389 biomolecules concentration and their steady state level with and without chemical  
390 exposure marking the difference between the normal and altered biology of the  
391 pathway.

392 The integrated PBPK/PD- coupled mechanistic system model well describes the  
393 observed changes in endogenous molecules level during and after discontinuation of  
394 exposure to the chemical. It can predict the adverse effect of environment chemicals  
395 considering both; the nature of changes in the system (altered biology) with respect to

396 normal biology, and, the capability of an endogenous molecule to retain homeostasis,  
397 mimicking the real in vivo physiological scenario. Therefore, this kind of model  
398 (integrated PBPK/PD- coupled mechanistic system model) can predict risk in more  
399 quantitatively as well as mechanistically considering pharmacokinetic,  
400 pharmacodynamic and relative altered biology from normal biology pathway as a  
401 consequence of chemical exposure. The advantage of Coupled integrated PBPK/PD-  
402 mechanistic system model is; it provides more understanding towards risk not only  
403 based on the target tissue concentration but also their effect on the target molecule  
404 participating in the biological network. Integrated PBPK/PD coupled mechanistic model  
405 are able to predict endogenous molecule concentration involved in pathway over their  
406 time course as a function of chemical exposure, which was shown by current developed  
407 model as a case study for PFOS

408 In summary, a molecular/cellular model that presented in this article mechanistically  
409 links BDNF involved in directed neuronal growth and neuronal survival, two distinct  
410 neurodevelopmental processes that use an overlapping molecular (that is genetic)  
411 machinery. The model does not provide further insights into which of these  
412 neurodevelopmental processes would be most relevant to the etiology of neurotoxicity,  
413 or where in the brain these processes are localized to selectively impact on neural  
414 circuitry. Although epigenetically regulation of BDNF (Lubin et al., 2008) in the brain  
415 by miRNA is very important were observed from literature in the theoretical network, it  
416 is unlikely that there would just be a single explanatory model that connects to BDNF  
417 on a molecular level and corresponding neuronal adverse outcomes. Rather, several  
418 etiological cascades contributing to neuronal adverse outcome are likely to exist.  
419 However, the currently developed model considered the following pathway for a series  
420 of signaling cascade biomolecules such as chemicals-miRNA-mRNA-RISCm-BDNF-  
421 neuronal survivability, previously described in the conceptual model (figure 2). For the  
422 currently selected pathway model predicts BDNF as a very sensitive endogenous  
423 species biomolecule, which maintains the cell survivability at steady state. Although,  
424 PFOS does not directly target BDNF in our model it still remains the sensitive target  
425 which could be due to its regulation is highly dependent on miRNA level. Comparison  
426 of figure 9 and 10 allow us to see the decrease in neuronal survivability (figure 10) is  
427 highly sensitive towards BDNF level (figure 9). The model shows that BDNF regulation  
428 (miRNA based regulation) is very much important for neuronal cell survivability. This  
429 shows BDNF could be an interesting species (biomarker) which can link between both  
430 environmental exposure and neuronal adverse outcomes.

431 There was an assumption of the existence of an empirical relation between the in-vitro  
432 toxicity to in-vivo toxicity (Wambaugh et al., 2013). Moreover, tools have been  
433 developed to translate in-vitro toxicity dose-response to predict the in-vivo toxicity by  
434 applying reverse dosimetry concept that provides equivalent in-vivo dose required to  
435 produce in-vitro toxicity, eventually validation of model was done by comparing POD  
436 (point of departure) from predicted in vivo dose response with reported POD of  
437 chemicals (Abdullah et al., 2016; Forsby and Blaauboer, 2007; Louisse et al., 2016;  
438 Wambaugh et al., 2013). In this case study of PFOS model (PBPK/PD coupled  
439 mechanistic model) due to lack of in-vivo data particularly for the following proposed  
440 mechanistic pathway, in worst case scenario we constrained to in-vitro data for  
441 qualitative or partial validation of the developed model. To check the performance of  
442 the developed PBPK/PD coupled mechanistic model, neuronal cell survivability was  
443 selected as an end point. Two approaches were used for this purpose; first  
444 reconstructing oral in-vivo equivalent dose for an in-vitro dose; second, response data

445 are generated for identified in vivo doses by mapping in vitro toxicity data (in this case  
446 neuronal cell survivability). Figure 10 illustrates, the simulated response variable (%  
447 neuronal survivability), for dose equivalent to in-vitro conc., vs observed linear  
448 interpolated response variable. Although model could not able to predict all the  
449 observed data, however, most of them were within the simulated range. The simulated  
450 maximum % of neuronal cell survivability on the lower side was around 35%, which is  
451 higher than the experimental observation of around 16 to 20%. This could be possibly  
452 explained by several facts such as current model uses adaptability mechanism which  
453 lacks in the in-vitro system, only one pathway has been accounted, neglecting the  
454 possibility of several mechanisms, empirical estimation of PFOS-miRNA interaction  
455 and the inherent uncertainty in in-vitro data and model.

456 The purpose of this work was to develop a simple model which combines  
457 pharmacokinetic model like PBPK predicting the internal tissue dosimetry and  
458 mechanistic system model via quantifying the Pharmacodynamic interaction of  
459 chemicals with key biomolecule components involved in the mechanistic system of  
460 biology. The measurement of mi-RNA, mRNA, BDNF in the brain at different time  
461 points gives evidence in parallel changes and difference in between them; significantly  
462 improves the understanding of relation with neuronal adverse outcomes. Here in this  
463 model, the mechanistic pathway can be considered as an equivalent AOP pathway for  
464 neurotoxicity. However, this can be further extended by integrating identified new  
465 pathways responsible for neurotoxicity. There are many ways that model can be  
466 extended to increase its utility, but certainly, the mi-RNA-based post-transcription  
467 regulation of BDNF not limited to PFOS. The same concept can be further applied to  
468 other environmental chemicals altering the similar system.

469 In this paper, we have partially validated our model, considering our objective of this  
470 paper is to focus on the illustration of tools that use simple integrated PBPK/PD-  
471 coupled mechanistic pathway model involving three main steps 1. Development of  
472 PBPK model, 2. Development of mechanistic system model 3. Couple PBPK with the  
473 mechanistic model by integrating PD model that quantify perturbed biomolecule (a  
474 component of the mechanistic model) as a result of chemical exposure. This step  
475 developed a new framework that could utilize the existing normal mechanistic pathways  
476 model and integrated PBPK/PD model, a step towards system toxicology based models.

#### 477 **Acknowledgement**

478 Preparation of this manuscript was supported in part for European Union's projects,  
479 HEALS (Health and Environment-wide Associations via Large population Surveys) by  
480 the FP7 Programme under grant agreement no. 603946 and EuroMix (European Test  
481 and Risk Assessment Strategies for Mixtures) by the Horizon 2020 Framework  
482 Programme under grant agreement no. 633172. Raju Prasad Sharma has received a  
483 doctoral fellowship from Universitat Rovira i Virgili under Martí-Franquès Research  
484 Grants Programme. This publication reflects only the authors' views. The Community  
485 and other funding organizations are not liable for any use made of the information  
486 contained therein.

#### 487 **References**

488 Abdullah, R., Alhusainy, W., Woutersen, J., Rietjens, I.M.C.M., Punt, A., 2016.  
489 Predicting points of departure for risk assessment based on in vitro cytotoxicity  
490 data and physiologically based kinetic (PBK) modeling: The case of kidney

- 491 toxicity induced by aristolochic acid I. *Food Chem. Toxicol.* 92, 104–116.  
492 doi:10.1016/j.fct.2016.03.017
- 493 Aderem, A., 2005. Systems biology: Its practice and challenges. *Cell* 121, 511–513.  
494 doi:10.1016/j.cell.2005.04.020
- 495 Andersen, M.E., Krewski, D., 2009. Toxicity testing in the 21st century: Bringing the  
496 vision to life. *Toxicol. Sci.* 107, 324–330. doi:10.1093/toxsci/kfn255
- 497 Andersen, M.E., Thomas, R.S., Gaido, K.W., Conolly, R.B., 2005. Dose-response  
498 modeling in reproductive toxicology in the systems biology era. *Reprod. Toxicol.*  
499 19, 327–337. doi:10.1016/j.reprotox.2004.12.004
- 500 Arrell, D.K., Terzic, a, 2010. Network systems biology for drug discovery. *Clin.*  
501 *Pharmacol. Ther.* 88, 120–125. doi:10.1038/clpt.2010.91
- 502 Auffray, C., Chen, Z., Hood, L., 2009. Systems medicine: the future of medical  
503 genomics and healthcare. *Genome Med.* 1, 2. doi:10.1186/gm2
- 504 Bartel, D.P., 2004. MicroRNAs: Genomics, Biogenesis, Mechanism, and Function. *Cell*  
505 116, 281–297. doi:10.1016/S0092-8674(04)00045-5
- 506 Bartlett, D.W., Davis, M.E., 2006. Insights into the kinetics of siRNA-mediated gene  
507 silencing from live-cell and live-animal bioluminescent imaging. *Nucleic Acids*  
508 *Res.* 34, 322–333. doi:10.1093/nar/gkj439
- 509 Bhattacharya, S., Shoda, L.K.M., Zhang, Q., Woods, C.G., Howell, B.A., Siler, S.Q.,  
510 Woodhead, J.L., Yang, Y., McMullen, P., Watkins, P.B., Melvin, E.A., 2012.  
511 Modeling drug- and chemical-induced hepatotoxicity with systems biology  
512 approaches. *Front. Physiol.* 3 DEC, 1–18. doi:10.3389/fphys.2012.00462
- 513 Bonate, P.L., 2011. *Pharmacokinetic-Pharmacodynamic Modeling and Simulation.*  
514 Springer US, Boston, MA. doi:10.1007/978-1-4419-9485-1
- 515 Boulle, F., van den Hove, D.L. a, Jakob, S.B., Rutten, B.P., Hamon, M., van Os, J.,  
516 Lesch, K.-P., Lanfumey, L., Steinbusch, H.W., Kenis, G., Hove, D.L.A. Van Den,  
517 Jakob, S.B., Rutten, B.P., Hamon, M., Os, J. Van, Lesch, K.-P., van den Hove,  
518 D.L. a, Jakob, S.B., Rutten, B.P., Hamon, M., van Os, J., Lesch, K.-P., Lanfumey,  
519 L., Steinbusch, H.W., Kenis, G., 2012. Epigenetic regulation of the BDNF gene:  
520 implications for psychiatric disorders. *Mol. Psychiatry* 17, 584–596.  
521 doi:10.1038/mp.2011.107
- 522 Bursac, N., Kirkton, R.D., Mcspadden, L.C., Liao, B., 2010. Circulating levels of brain-  
523 derived neurotrophic factor: correlation with mood, cognition and motor function.  
524 *Biomark. Med.* 4, 871–87.
- 525 Calabrese, E.J., Baldwin, L.A., 2003. Toxicology rethinks its central belief. *Nature* 421,  
526 691–692. doi:10.1038/421691a
- 527 Caputo, V., Sinibaldi, L., Fiorentino, A., Parisi, C., Catalanotto, C., Pasini, A., Cogoni,  
528 C., Pizzuti, A., 2011. Brain derived neurotrophic factor (BDNF) expression is  
529 regulated by microRNAs miR-26a and miR-26b allele-specific binding. *PLoS One*  
530 6. doi:10.1371/journal.pone.0028656

- 531 Carlotti, F., Dower, S.K., Qvarnstrom, E.E., 2000. Dynamic shuttling of nuclear  
532 factor  $\beta$  between the nucleus and cytoplasm as a consequence of inhibitor  
533 dissociation. *J. Biol. Chem.* 275, 41028–41034. doi:10.1074/jbc.M006179200
- 534 Castillo, B., del Cerro, M., Breakefield, X.O., Frim, D.M., Barnstable, C.J., Dean, D.O.,  
535 Bohn, M.C., 1994. Retinal ganglion cell survival is promoted by genetically  
536 modified astrocytes designed to secrete brain-derived neurotrophic factor (BDNF).  
537 *Brain Res.* 647, 30–36. doi:10.1016/0006-8993(94)91395-1
- 538 Chen, N., Li, J., Li, D., Yang, Y., He, D., 2014. Chronic exposure to perfluorooctane  
539 sulfonate induces behavior defects and neurotoxicity through oxidative damages,  
540 in Vivo and in Vitro. *PLoS One* 9, 1–10. doi:10.1371/journal.pone.0113453
- 541 Clarke, G., Collins, R.A., Leavitt, B.R., Andrews, D.F., Hayden, M.R., Lumsden, C.J.,  
542 McInnes, R.R., 2000. A one-hit model of cell death in inherited neuronal  
543 degenerations. *Nature* 406, 195–199. doi:10.1038/35018098
- 544 Djuranovic, S., Nahvi, A., Green, R., 2011. A Parsimonious Model for Gene Regulation  
545 by miRNAs. *Science* (80-. ). 331, 550–553. doi:10.1126/science.1191138
- 546 Fabrega, F., Kumar, V., Schuhmacher, M., Domingo, J.L., Nadal, M., 2014. PBPK  
547 modeling for PFOS and PFOA: Validation with human experimental data. *Toxicol.*  
548 *Lett.* 230, 244–251. doi:10.1016/j.toxlet.2014.01.007
- 549 Fàbrega, F., Nadal, M., Schuhmacher, M., Domingo, J.L., Kumar, V., 2016. Influence  
550 of the uncertainty in the validation of PBPK models: A case-study for PFOS and  
551 PFOA. *Regul. Toxicol. Pharmacol.* 77, 230–239. doi:10.1016/j.yrtph.2016.03.009
- 552 Fletcher, J.M., Morton, C.J., Zwar, R.A., Murray, S.S., O’Leary, P.D., Hughes, R.A.,  
553 2008. Design of a conformationally defined and proteolytically stable circular  
554 mimetic of brain-derived neurotrophic factor. *J. Biol. Chem.* 283, 33375–33383.  
555 doi:10.1074/jbc.M802789200
- 556 Forsby, A., Blaauboer, B., 2007. Integration of in vitro neurotoxicity data with  
557 biokinetic modelling for the estimation of in vivo neurotoxicity. *Hum. Exp.*  
558 *Toxicol.* 26, 333–338. doi:10.1177/0960327106072994
- 559 Foxenberg, R.J., Ellison, C.A., Knaak, J.B., Ma, C., Olson, J.R., 2011. Cytochrome  
560 P450-specific human PBPK/PD models for the organophosphorus pesticides:  
561 Chlorpyrifos and parathion. *Toxicology* 285, 57–66. doi:10.1016/j.tox.2011.04.002
- 562 Fukumitsu, H., Ohtsuka, M., Murai, R., Nakamura, H., Itoh, K., Furukawa, S., 2006.  
563 Brain-Derived Neurotrophic Factor Participates in Determination of Neuronal  
564 Laminar Fate in the Developing Mouse Cerebral Cortex. *J. Neurosci.* 26, 13218–  
565 13230. doi:10.1523/JNEUROSCI.4251-06.2006
- 566 Gatzeva-topalova, P.Z., Warner, L.R., Pardi, A., Carlos, M., 2011. NIH Public Access  
567 18, 1492–1501. doi:10.1016/j.str.2010.08.012.Structure
- 568 Gillespie, L.N., Clark, G.M., Bartlett, P.F., Marzella, P.L., 2003. BDNF-induced  
569 survival of auditory neurons in vivo: Cessation of treatment leads to accelerated  
570 loss of survival effects. *J. Neurosci. Res.* 71, 785–790. doi:10.1002/jnr.10542
- 571 Gim, J., Kim, H.S., Kim, J., Choi, M., Kim, J.R., Chung, Y.J., Cho, K.H., 2010. A

- 572 system-level investigation into the cellular toxic response mechanism mediated by  
573 AhR signal transduction pathway. *Bioinformatics* 26, 2169–2175.  
574 doi:10.1093/bioinformatics/btq400
- 575 Gohlke, J.M., Griffith, W.C., Faustman, E.M., 2005. A systems-based computational  
576 model for dose-response comparisons of two mode of action hypotheses for  
577 ethanol-induced neurodevelopmental toxicity. *Toxicol. Sci.* 86, 470–484.  
578 doi:10.1093/toxsci/kfi209
- 579 Goudarzi, H., Nakajima, S., Ikeno, T., Sasaki, S., Kobayashi, S., Miyashita, C., Ito, S.,  
580 Araki, A., Nakazawa, H., Kishi, R., 2016. Prenatal exposure to perfluorinated  
581 chemicals and neurodevelopment in early infancy: The Hokkaido Study. *Sci. Total*  
582 *Environ.* 541, 1002–1010. doi:10.1016/j.scitotenv.2015.10.017
- 583 Haley, B., Zamore, P.D., 2004. Kinetic analysis of the RNAi enzyme complex. *Nat.*  
584 *Struct. Mol. Biol.* 11, 599–606. doi:10.1038/nsmb780
- 585 Hood, L., Heath, J.R., Phelps, M.E., Lin, B., 2004. Systems biology and new  
586 technologies enable predictive and preventative medicine. *Science* 306, 640–643.  
587 doi:10.1126/science.1104635
- 588 Johansson, N., Fredriksson, A., Eriksson, P., 2008. Neonatal exposure to  
589 perfluorooctane sulfonate (PFOS) and perfluorooctanoic acid (PFOA) causes  
590 neurobehavioural defects in adult mice. *Neurotoxicology* 29, 160–169.  
591 doi:10.1016/j.neuro.2007.10.008
- 592 Kell, D.B., 2006. Systems biology, metabolic modelling and metabolomics in drug  
593 discovery and development. *Drug Discov. Today* 11, 1085–1092.  
594 doi:10.1016/j.drudis.2006.10.004
- 595 Kitano, H., 2002. Systems biology: A brief overview. *Sci. (New York, NY)* 295, 1662–  
596 1664. doi:10.1126/science.1069492
- 597 Kohler, J.J., Schepartz, A., 2001. Kinetic Studies of Fos , Jun , DNA Complex  
598 Formation : DNA Binding Prior to Dimerization. *Biochemistry* 40, 130–142.  
599 doi:10.1021/bi001881p
- 600 Li, W., He, Q.Z., Wu, C.Q., Pan, X.Y., Wang, J., Tan, Y., Shan, X.Y., Zeng, H.C.,  
601 2015. PFOS Disturbs BDNF-ERK-CREB Signalling in Association with Increased  
602 MicroRNA-22 in SH-SY5Y Cells. *Biomed Res. Int.* 2015.  
603 doi:10.1155/2015/302653
- 604 Lipsky, R.H., Marini, A.M., 2007. Brain-derived neurotrophic factor in neuronal  
605 survival and behavior-related plasticity. *Ann. N. Y. Acad. Sci.* 1122, 130–143.  
606 doi:10.1196/annals.1403.009
- 607 Long, Y., Wang, Y., Ji, G., Yan, L., Hu, F., Gu, A., 2013. Neurotoxicity of  
608 Perfluorooctane Sulfonate to Hippocampal Cells in Adult Mice. *PLoS One* 8, 1–9.  
609 doi:10.1371/journal.pone.0054176
- 610 Lousse, J., Beekmann, K., Rietjens, I.M.C.M., 2016. Use of physiologically based  
611 kinetic modeling-based reverse dosimetry to predict in vivo toxicity from in vitro  
612 data. *Chem. Res. Toxicol.* *acs.chemrestox.6b00302.*  
613 doi:10.1021/acs.chemrestox.6b00302

- 614 Lu, B., 2003. Pro-Region of Neurotrophins. *Neuron* 39, 735–738. doi:10.1016/S0896-  
615 6273(03)00538-5
- 616 Lubin, F.D., Roth, T.L., Sweatt, J.D., 2008. Epigenetic regulation of BDNF gene  
617 transcription in the consolidation of fear memory. *J. Neurosci.* 28, 10576–86.  
618 doi:10.1523/JNEUROSCI.1786-08.2008
- 619 Ma, E., MacRae, I.J., Kirsch, J.F., Doudna, J.A., 2008. Autoinhibition of Human Dicer  
620 by Its Internal Helicase Domain. *J. Mol. Biol.* 380, 237–243.  
621 doi:10.1016/j.jmb.2008.05.005
- 622 Menei, P., Montero-Menei, C., Whittemore, S.R., Bunge, R.P., Bunge, M.B., 1998.  
623 Schwann cells genetically modified to secrete human BDNF promote enhanced  
624 axonal regrowth across transected adult rat spinal cord. *Eur. J. Neurosci.* 10, 607–  
625 621. doi:10.1046/j.1460-9568.1998.00071.x
- 626 Michael, G.J., Averill, S., Nitkunan, A., Rattray, M., Bennett, D.L., Yan, Q., Priestley,  
627 J. V., 1997. Nerve growth factor treatment increases brain-derived neurotrophic  
628 factor selectively in TrkA-expressing dorsal root ganglion cells and in their central  
629 terminations within the spinal cord. *J. Neurosci.* 17, 8476–90.
- 630 Mowla, S.J., Pareek, S., Farhadi, H.F., Petrecca, K., Fawcett, J.P., Seidah, N.G., Morris,  
631 S.J., Sossin, W.S., Murphy, R. a, 1999. Differential sorting of nerve growth factor  
632 and brain-derived neurotrophic factor in hippocampal neurons. *J. Neurosci.* 19,  
633 2069–2080.
- 634 Muiños-Gimeno, M., Espinosa-Parrilla, Y., Guidi, M., Kagerbauer, B., Sipilä, T.,  
635 Maron, E., Pettai, K., Kananen, L., Navinés, R., Martín-Santos, R., Gratacòs, M.,  
636 Metspalu, A., Hovatta, I., Estivill, X., 2011. Human microRNAs miR-22, miR-  
637 138-2, miR-148a, and miR-488 are associated with panic disorder and regulate  
638 several anxiety candidate genes and related pathways. *Biol. Psychiatry* 69, 526–  
639 533. doi:10.1016/j.biopsych.2010.10.010
- 640 Murer, M., Yan, Q., Raisman-Vozari, R., 2001. Brain-derived neurotrophic factor in  
641 the control human brain, and in Alzheimer’s disease and Parkinson’s disease. *Prog.*  
642 *Neurobiol.* 63, 71–124. doi:10.1016/S0301-0082(00)00014-9
- 643 O’Leary, P.D., Hughes, R.A., 1998. Structure-activity relationships of conformationally  
644 constrained peptide analogues of loop 2 of brain-derived neurotrophic factor. *J.*  
645 *Neurochem.* 70, 1712–21. doi:10.1046/j.1471-4159.1998.70041712.x
- 646 Pérez-Ortín, J.E., Alepuz, P.M., Moreno, J., 2007. Genomics and gene transcription  
647 kinetics in yeast. *Trends Genet.* 23, 250–257. doi:10.1016/j.tig.2007.03.006
- 648 Perruisseau-Carrier, C., Jurga, M., Forraz, N., McGuckin, C.P., 2011. MiRNAs stem  
649 cell reprogramming for neuronal induction and differentiation. *Mol. Neurobiol.* 43,  
650 215–227. doi:10.1007/s12035-011-8179-z
- 651 Rodríguez-Tébar, A., Dechant, G., Götz, R., Barde, Y.A., 1992. Binding of  
652 neurotrophin-3 to its neuronal receptors and interactions with nerve growth factor  
653 and brain-derived neurotrophic factor. *EMBO J.* 11, 917–922.
- 654 Sandhya, V.K., Raju, R., Verma, R., Advani, J., Sharma, R., Radhakrishnan, A.,  
655 Nanjappa, V., Narayana, J., Somani, B.L., Mukherjee, K.K., Pandey, A.,

- 656 Christopher, R., Keshava Prasad, T.S., 2013. A network map of BDNF/TRKB and  
657 BDNF/p75NTR signaling system. *J. Cell Commun. Signal.* 7, 301–307.  
658 doi:10.1007/s12079-013-0200-z
- 659 Sato, I., Kawamoto, K., Nishikawa, Y., Tsuda, S., Yoshida, M., Yaegashi, K., Saito, N.,  
660 Liu, W., Jin, Y., 2009. Neurotoxicity of perfluorooctane sulfonate (PFOS) in rats  
661 and mice after single oral exposure. *J. Toxicol. Sci.* 34, 569–574.  
662 doi:10.2131/jts.34.569
- 663 Thiel, C., Cordes, H., Conde, I., Castell, J.V., Blank, L.M., Kuepfer, L., 2017. Model-  
664 based contextualization of in vitro toxicity data quantitatively predicts in vivo drug  
665 response in patients. *Arch. Toxicol.* 91, 865–883. doi:10.1007/s00204-016-1723-x
- 666 Timchalk, C., Nolan, R.J., Mendrala, A.L., Dittenber, D.A., Brzak, K.A., Mattsson, J.L.,  
667 2002. A physiologically based pharmacokinetic and pharmacodynamic (PBPK/PD)  
668 model for the organophosphate insecticide chlorpyrifos in rats and humans.  
669 *Toxicol. Sci.* 66, 34–53. doi:10.1093/toxsci/66.1.34
- 670 Vuong, A.M., Yolton, K., Webster, G.M., Sjödin, A., Calafat, A.M., Braun, J.M.,  
671 Dietrich, K.N., Lanphear, B.P., Chen, A., 2016. Prenatal polybrominated diphenyl  
672 ether and perfluoroalkyl substance exposures and executive function in school-age  
673 children. *Environ. Res.* 147, 556–564. doi:10.1016/j.envres.2016.01.008
- 674 Wambaugh, J.F., Setzer, R.W., Pitruzzello, A.M., Liu, J., Reif, D.M., Kleinstreuer,  
675 N.C., Wang, N.C.Y., Sipes, N., Martin, M., Das, K., DeWitt, J.C., Strynar, M.,  
676 Judson, R., Houck, K.A., Lau, C., 2013. Dosimetric anchoring of In vivo and In  
677 vitro studies for perfluorooctanoate and perfluorooctanesulfonate. *Toxicol. Sci.*  
678 136, 308–327. doi:10.1093/toxsci/kft204
- 679 Wang, X., Li, Y., Xu, X., Wang, Y. hua, 2010. Toward a system-level understanding of  
680 microRNA pathway via mathematical modeling. *BioSystems* 100, 31–38.  
681 doi:10.1016/j.biosystems.2009.12.005
- 682 Waters, M.D., Boorman, G., Bushel, P., Cunningham, M., Irwin, R., Merrick, A.,  
683 Olden, K., Paules, R., Selkirk, J., Stasiewicz, S., Weis, B., Van Houten, B.,  
684 Walker, N., Tennant, R., 2003. Systems toxicology and the Chemical Effects in  
685 Biological Systems (CEBS) knowledge base. *Environ. Health Perspect.* 111, 811–  
686 824. doi:10.1289/txg.5971
- 687 Yang, J., Wang, C., Nie, X., Shi, S., Xiao, J., Ma, X., Dong, X., Zhang, Y., Han, J., Li,  
688 T., Mao, J., Liu, X., Zhao, J., Wu, Q., 2015. Perfluorooctane sulfonate mediates  
689 microglial activation and secretion of TNF- $\alpha$  through Ca<sup>2+</sup>-dependent PKC-NF-  
690  $\kappa$ B signaling. *Int. Immunopharmacol.* 28, 52–60. doi:10.1016/j.intimp.2015.05.019
- 691 York, N., 2015. Regulation of Cell Survival by Secreted Proneurotrophins.pdf. *Science*  
692 (80-. ). 294, 1945–1949. doi:10.1126/science.1065057
- 693 You, H.J., Park, J.H., Pareja-Galeano, H., Lucia, A., Shin, J. Il, 2016. Targeting  
694 MicroRNAs Involved in the BDNF Signaling Impairment in Neurodegenerative  
695 Diseases. *NeuroMolecular Med.* doi:10.1007/s12017-016-8407-9
- 696 Yu, N., Wei, S., Li, M., Yang, J., Li, K., Jin, L., Xie, Y., Giesy, J.P., Zhang, X., Yu, H.,  
697 2016. Effects of Perfluorooctanoic Acid on Metabolic Profiles in Brain and Liver

698 of Mouse Revealed by a High-throughput Targeted Metabolomics Approach. *Sci.*  
699 *Rep.* 6, 23963. doi:10.1038/srep23963

700 Zeng, H. cai, Zhang, L., Li, Y. yuan, Wang, Y. jian, Xia, W., Lin, Y., Wei, J., Xu, S.  
701 qing, 2011. Inflammation-like glial response in rat brain induced by prenatal PFOS  
702 exposure. *Neurotoxicology* 32, 130–139. doi:10.1016/j.neuro.2010.10.001

703 Zhang, L., Li, Y.-Y., Zeng, H.-C., Wei, J., Wan, Y.-J., Chen, J., Xu, S.-Q., 2011.  
704 MicroRNA expression changes during zebrafish development induced by  
705 perfluorooctane sulfonate. *J. Appl. Toxicol.* 31, 210–222. doi:10.1002/jat.1583

706 Zhao, Y., Ricci, P.F., 2010. Modeling dose-response at low dose: A systems biology  
707 approach for ionization radiation. *Dose-Response* 8, 456–477. doi:10.2203/dose-  
708 response.09-054.Zhao

709

710

711

712

713 **Figure Labels**

714 Figure 1. describes the miRNA-mRNA-BDNF-cell survival mechanistic pathway  
715 showing the importance of miRNA in regulating BDNF via forming a complex with  
716 RNA-induced silencing complex. Later BDNF binding to TrkB with the sequential  
717 activation of pathway **such as MAPK/ERK and PI3K/AKT causing increase in**  
718 **CREB expression which leads to increase in** neuronal survival, differentiation, and  
719 proliferation.

720 Figure 2. represents the full scheme of PBPK/PD model showing the integration of  
721 tissue dosimetry model with miRNA-BDNF-Cell survival pathway via  
722 pharmacodynamic interaction of PFOS-miRNA.

723 Figure 3. Schema for the estimation of in-vivo oral dose

724 Figure 5. Simulated brain concentrations of PFOS over the time period. The figure  
725 shows a simulation of the time course of PFOS concentration in the brain for each 12  
726 different doses corresponding to in-vitro dose. The single oral dose was given at 240hr.

727 Figure 4. represents the pharmacodynamic interaction of PFOS-miRNA and the  
728 consequent effect on neuronal survivability rate.

729 Figure 6. Mechanistic Base model. The figure shows simulated key biomolecules such  
730 as RISC, miRNA, RISCm, BDNF and percentage neuronal cell survivability.

731 Figure 7. simulated time vs miRNA level The figure depicts simulated miRNA  
732 concentration after single oral dose of PFOS for 12 different dose levels.

733 Figure 8. Simulated time vs RISCm level. The figure shows the increase in RISCm  
734 level after single oral dose of PFOS for 12 different dose levels.

735 Figure 9. Simulated time vs BDNF level. The figure depicts simulated BDNF  
736 concentration after single oral dose of PFOS for 12 different dose levels.

737 Figure 10. Simulated vs predicted neuronal cell survivability (percentage). The figure  
738 depicts simulated vs observed neuronal cell survivability (percentage) after single oral  
739 dose of PFOS for 12 different dose levels.

740

## 741 TABLES

742 Table 1. oral equivalent dose calculated based on AUC extrapolation method

in-vitro dose ( $\mu\text{M}$ )	AUC_24 (nM*hr)	AUC_48 (nM*hr)	in-vivo dose (nM)(24hr)	in-vivo dose (nM) (48hr)
1	24000	48000	86925	130570
10	240000	480000	896550	1362850
50	1200000	2400000	4494910	6839718
100	2400000	4800000	8992868	13685810
150	3600000	7200000	13490820	20531899
200	4800000	9600000	17988780	27378025

743

744 Table 2. Scaled parameters for Coupled PBPK/PD mechanistic pathway model

Description	Parameter Symbol	Value	References
BDNF synthesis rate	Kin_BDNF	.023 nM/hr/kg 0.75	(Menei et al., 1998)
BDNF dissipation rate	Kout_BDNF	0.231/hr	(Fukumitsu et al., 2006)
Maximum BDNF effect on cell survival	E <sub>max</sub>	100	Assumed
Half maximum concentration of BDNF for neuron survivability	EC <sub>50</sub> _BDNF	5E-03 nM	(O'Leary and Hughes, 1998)
Cell degradation constant	K <sub>d</sub> _cell	2.45e-5/hr	(Clarke et al., 2000)
Maximum PFOS effect on miRNA	E <sub>max</sub> _miRNA	2.4	maximum fold change(Li et al., 2015)
Half maximum stimulatory concentration of PFOS for miRNA	EC <sub>50</sub> _PFOS	1000nM	(Li et al., 2015)
Volume of cytoplasm	V_cyt	4e-12/L	(Bartlett and Davis, 2006)
Volume of nucleus	V_nucleus	4e-13	(Carlotti et al., 2000)
Pri miRNA synthesis rate	K_primiRNA	3.6 nM/hr	(Pérez-Ortín et al., 2007)
mRNA synthesis rate	K_mRNA	0.36 nM/hr	(Bartlett and Davis, 2006)
Adjusted Coefficient of R promoting pri-miRNA maturation	R_miRNA	0.001 nM	(Wang et al., 2010)

<b>pri-miRNA to pre-miRNA(n) catalyzed by R</b>	<b>K_primiRNA-premiRNA</b>	<b>360/hr</b>	(Wang et al., 2010)
<b>premiRNA transport rate</b>	<b>T_premiRNA</b>	<b>180/hr</b>	(Wang et al., 2010)
<b>Rate of premiRNA(c) conversion to dsRNA</b>	<b>K_premiRNA-dsRNA</b>	<b>36/hr</b>	(Ma et al., 2008)
<b>miRNA formation rate</b>	<b>K_miRNA</b>	<b>36/hr</b>	(Kohler and Schepartz, 2001)
<b>miRNA-induced RISC formation rate</b>	<b>K_RISC</b>	<b>108/hr</b>	(Bartlett and Davis, 2006)
<b>mRNA-RISC complex formation rate</b>	<b>K_[mRNA-RISC]</b>	<b>3.6nM/hr</b>	(Haley and Zamore, 2004)
<b>mRNA cleavage rate</b>	<b>Kc_mRNA</b>	<b>25.27</b>	(Haley and Zamore, 2004)
<b>Dissociation rate of RISC complex</b>	<b>Kd_[mRNA-RISC]</b>	<b>3.6/hr</b>	(Wang et al., 2010)
<b>Rate of pri-miRNA degradation</b>	<b>d_primiRNA</b>	<b>0.9/hr</b>	(Wang et al., 2010)
<b>Rate of pre-miRNA(c) degradation</b>	<b>d_premiRNA</b>	<b>0.9/hr</b>	(Wang et al., 2010)
<b>Rate of dsRNA degradation</b>	<b>d_dsRNA</b>	<b>3.96/hr</b>	(Wang et al., 2010)
<b>Rate of miRNA degradation</b>	<b>d_miRNA</b>	<b>0.9/hr</b>	(Wang et al., 2010)
<b>Rate of RISC degradation</b>	<b>d_RISC</b>	<b>0.36/hr</b>	(Wang et al., 2010)
<b>Rate of mRNA-bound RISC complex degradation</b>	<b>d_[mRNA-RISC]</b>	<b>0.077/hr</b>	(Wang et al., 2010)
<b>Rate of mRNA degradation</b>	<b>d_mRNA</b>	<b>0.36/hr</b>	(Wang et al., 2010)